

# Ultra-cold mechanical resonators coupled to atoms in an optical lattice

Andrew A. Geraci\* and John Kitching

*Time and Frequency Division, National Institute of Standards and Technology, Boulder, CO 80305 USA*

(Dated: November 7, 2018)

We propose an experiment utilizing an array of cooled micro-cantilevers coupled to a sample of ultra-cold atoms trapped near a micro-fabricated surface. The cantilevers allow individual lattice site addressing for atomic state control and readout, and potentially may be useful in optical lattice quantum computation schemes. Assuming resonators can be cooled to their vibrational ground state, the implementation of a two-qubit controlled-NOT gate with atomic internal states and the motional states of the resonator is described. We also consider a protocol for entangling two or more cantilevers on the atom chip with different resonance frequencies, using the trapped atoms as an intermediary. Although similar experiments could be carried out with magnetic microchip traps, the optical confinement scheme we consider may exhibit reduced near-field magnetic noise and decoherence. Prospects for using this novel system for tests of quantum mechanics at macroscopic scales or quantum information processing are discussed.

PACS numbers: 37.10.Jk,03.67.-a,07.10.Cm

Over the past decade, significant research effort has been undertaken to realize the cooling of a macroscopic mechanical resonator to its vibrational ground state [1, 2, 3, 4, 5, 6, 7, 8]. Given the recent experimental progress in this field, ground state cooling will likely be achieved within the next few years, and investigating the quantum coherence in mechanical resonators [9, 10] will then become an exciting and important new field of research, as the boundary between quantum microscopic phenomena and macroscopic systems breaks down.

A natural method to study the quantum coherence in these macroscopic systems is to observe their coupling to other quantum systems with well understood coherence properties, for example, a two-level system such as a Cooper-pair box [11], superconducting flux qubit [12], or nitrogen-vacancy (NV) impurity in diamond [13]. Ultra-cold atoms represent another prime example of microscopic quantum coherence, exhibiting long coherence times. They can be used for quantum control, and can be trapped at sub-micrometer distance from a surface [14]. It has recently been pointed out that magnetic cantilevers can couple to ultra-cold atoms at micrometer distances in a regime analogous to the strong coupling regime of cavity quantum electrodynamics [15], enabling studies of decoherence and quantum control.

Trapped atoms can be arranged in regular, transportable arrays via optical lattice potentials [16]. Cantilevers, on the other hand, can be precisely defined on the surface of a chip with lithography, and can be scaled into large two-dimensional arrays. In this paper, we propose an experiment involving neutral atoms in selectively occupied sites of an optical lattice near a surface, coupled via the Zeeman interaction  $H_{\text{int}} = -\vec{\mu} \cdot \vec{B}$  to a matched array of cooled magnetic micro-cantilevers residing underneath. Unlike superconducting qubits or NV centers, the atomic system has the feature that the atoms are identical, and affords flexibility in that the atomic magnetic resonances can be widely tuned with a magnetic field to

match the cantilever mechanical resonances. Also, the atoms can in principle be transported to interact locally with multiple individual cantilevers.

Driven magnetic resonance in a  $^{87}\text{Rb}$  atomic vapor has been experimentally demonstrated with a magnetic micro-resonator [17], and similar experiments are currently underway for trapped cold-atoms [15]. The demonstrated high force sensitivity of micro-cantilevers, for example enabling single spin detection in solids [18], makes individual atom Zeeman state detection possible at sub-micron distances. Such capabilities may be useful for individual lattice site addressing in neutral-atom optical-lattice quantum information processing [19, 20, 21].

The proposed experimental setup is shown in Fig. 1. The cantilevers have dimensions  $l = 8 \mu\text{m}$ ,  $w = 0.2 \mu\text{m}$ , and  $t = 0.1 \mu\text{m}$  and are separated from the 3-dimensional atomic optical lattice by a 120 nm thin mirror membrane coated with 30 nm Pt. The atoms are trapped in a 2-d array at distance  $d = 100 - 400 \text{ nm}$  below the surface. We henceforth consider a one-dimensional lattice of atoms and cantilevers in the  $x$  direction. In principle many such arrays can be used in parallel to form a two-dimensional lattice. The cantilevers carry a rectangular nano-magnet with strong magnetization  $M = 10^6 \text{ A/m}$ , attainable in thin-film magnets, and dimensions  $700 \times 200 \times 150 \text{ nm}$  in the  $x, y$  and  $z$  directions, respectively. We assume a single magnetic domain with moment in the  $x$ -direction determined by the shape anisotropy. The fundamental-mode resonance frequency of the loaded cantilever is  $\omega_c/2\pi = 1.1 \text{ MHz}$ . Additional gradient compensation magnets of  $x, y, z$  dimensions of  $5.1 \mu\text{m} \times 200 \text{ nm} \times 150 \text{ nm}$  are located on either side of the cantilevers with a  $x$ -separation of 100 nm to minimize the magnetic gradient at the optical potential minimum. We take an optical lattice with  $\lambda_{\text{eff}} = 1500 \text{ nm}$ , and depth 500 times the photon-recoil energy  $E_r$ , corresponding to a trap frequency  $\omega_t/2\pi = 124 \text{ kHz}$ , and lattice spacing parameter

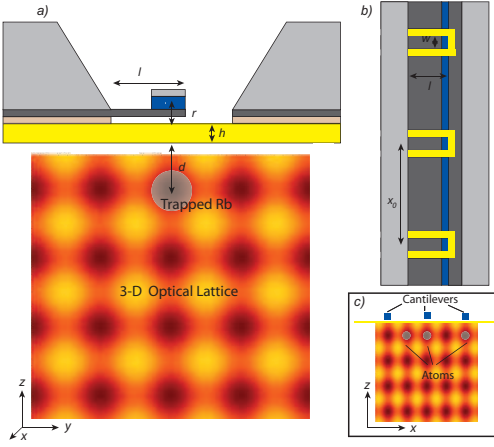


FIG. 1: (Color) Proposed experimental geometry. Here  $r = 250$  nm,  $h = 150$  nm, and the total atom-cantilever vertical separation  $z = r + h + d < 1$   $\mu\text{m}$ . The silicon cantilevers are horizontally separated by distance that is an integer multiple of the optical lattice spacing  $x_0 = j\lambda_{\text{eff}}/2$ . Magnetic cantilever tips and gradient compensation magnets are shown in blue. Bulk silicon providing structural support for the chip is shown in light gray. Mirror membrane is shown in yellow. a), b), and c) depict views from the  $x, z$ , and  $y$  directions, respectively.

$j = 8$ . For definiteness, we consider a configuration where the first vertical anti-node occurs at  $d = 375$  nm from the surface. An external bias field of  $B_x = 275$   $\mu\text{T}$  is applied to remove the residual  $B_x$  field for a sub-array of three cantilevers and their neighboring compensation magnets, and  $B_y = 160$   $\mu\text{T}$  is applied to set the desired magnetic field and quantization axis at the trap minimum, corresponding to a Larmor frequency  $\omega_L/2\pi$  of 1.1 MHz. The total potential is shown in Fig. 2. Tunneling towards the surface can result from the decreased potential well-depth due to the attractive Casimir-Polder interaction [22]. The deep optical lattice serves in part to prevent this loss mechanism, and to further avoid this loss, we operate with only weak magnetic field seeking states, for which the magnetic field from the cantilever tip provides a strong repulsive interaction.

For atomic state manipulation, a local AC voltage can be applied near a cantilever to drive its motion capacitively; the corresponding atomic Rabi frequency is proportional to the amplitude  $\delta z$  of this motion:  $\Omega_R = \frac{g_F G_m \mu_B \delta z}{\hbar}$  for tip magnetic gradient  $G_m$ . In order to coherently change internal atomic states, the cantilever can be driven into a large amplitude yielding a sufficiently large Rabi frequency so that the thermal motion has little effect over the period of a Rabi cycle. At distance  $a \gg d$  from the cantilever,  $G_m \propto a^{-4}$ , leading to highly localized interactions. In addition, differing mechanical frequencies can be used isolate neighboring sites.

The minimum detectable force due to thermal noise

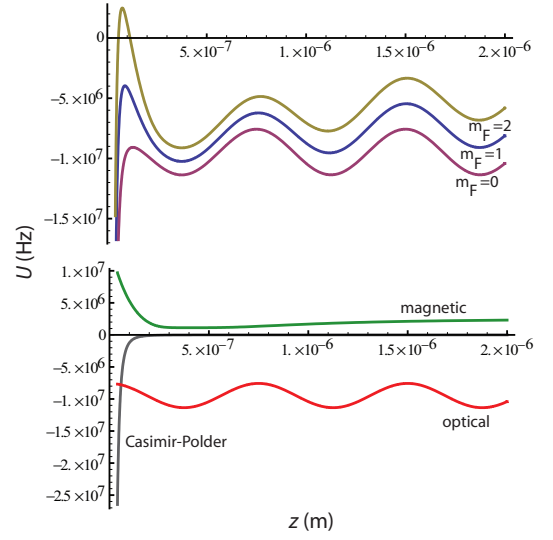


FIG. 2: (Color online) (Upper) Combined optical lattice, Casimir-Polder potential, gravitational potential, and magnetic potential of magnets and bias magnetic field as a function of vertical distance  $z$  from the surface for states  $|F = 2, m_F = 2\rangle \equiv |\text{aux}\rangle$ ,  $|F = 2, m_F = 1\rangle \equiv |\uparrow\rangle$ , and  $|F = 2, m_F = 0\rangle$ . (Lower) Magnetic potential for  $|\uparrow\rangle$ , Casimir-polder potential, and optical lattice shown separately.

at temperature  $T$  is  $F_{\text{min}} = \sqrt{\frac{4k k_B T b}{\omega_c Q}}$ , where  $k$  is the cantilever spring constant,  $\omega_c$  is the resonance frequency,  $Q$  is its quality factor, and  $b$  is the bandwidth of the measurement. For a cantilever separated from a single atom by a distance of 400 nm, the rms force from atomic spin precession is  $F_s = g_F \mu_B G_m / \sqrt{2} = 1.9 \times 10^{-19}$  N, becoming detectable in an integration time  $b^{-1}$  of 250 ms by a thermal cantilever at  $T = 10$  mK, with  $Q = 10^5$  and  $k = 0.012$  N/m.

If we set  $k_B T \approx \bar{N}_{\text{th}} \hbar \omega_c$  and  $b = \kappa \equiv \omega_c / 2Q$ , and require  $F_{\text{min}} < F_s$ , we obtain a limit on the phonon occupation number  $\bar{N}_{\text{th}}$  of the cantilever:  $\sqrt{\bar{N}_{\text{th}}} < \frac{\Omega_0 Q}{\sqrt{2}\omega_c}$  in order that the force be detected within the cantilever ring-down time  $2Q/\omega_c$ , where  $\Omega_0 \equiv g_F \mu_B G_m z_{qm} / \hbar$ . Here  $z_{qm} = \sqrt{\frac{\hbar}{2m_{\text{eff}}\omega_c}}$ , and  $m_{\text{eff}} \approx 0.24m_c + m_{\text{mag}}$ , where  $m_c$  is the mass of the Si cantilever and  $m_{\text{mag}}$  is the mass of the magnet. For example, if  $Q = 10^5$ ,  $\Omega_0 = 2\pi \times 10$  rad/s, and  $\omega_c = 2\pi \times 10^6$  rad/s, this requires  $\bar{N}_{\text{th}}$  of order 1, so the cantilever must be cooled near its ground state of motion. To facilitate single-atom detection with a thermal cantilever, an adiabatic fast passage protocol similar to that used in magnetic resonance force microscopy could be used [7]. A separate sub-lattice of lower frequency cantilevers could be used for this purpose, with atoms being transportable between this detection sub-lattice and the higher resonance frequency control sub-lattice discussed earlier. Here the detection cantilevers can operate at a frequency  $\sim 10$  kHz corresponding to

the sweep rate of the adiabatic fast passage, while the cantilevers in the control sub-lattice can still have resonances around 1 MHz as discussed earlier. To distinguish hyperfine levels in this approach, microwave near fields could be used, for example as proposed in Ref. [23].

*Optical lattice quantum computation.* Single site addressing remains a key challenge for neutral-atom optical-lattice quantum information scenarios. Although focused laser pulses may provide a solution [24], the cantilever approach is not limited by optical diffraction. As an example, we consider the SWAP gate recently realized in Ref. [25]. The setup consists of a two-dimensional optical lattice that can be transformed into double-wells. The internal qubit states used in the experiment are the  $m_F = 0$  and  $m_F = -1$  sublevels of the  $F = 1$  hyperfine ground state manifold of  $^{87}\text{Rb}$ . Here a vector light-shift provides an effective magnetic field that allows RF addressing of a sublattice to prepare and toggle these internal states. If the optical lattice can be formed near a surface with a lattice array of cantilevers underneath such as that described in this work, rather than using a global RF source for state preparation, individual driven magnetic cantilevers could be used, adding the capability of single-site state control. Cantilever arrays may be generally useful for single qubit operations in cluster-state quantum computation [20].

*Quantum gates and entanglement.* We now assume that the fundamental cantilever vibrational mode can be cooled to its ground state and that the measurement imprecision and back-action are sufficiently small that the zero-point cantilever motion can be detected, for example optically or capacitively from the reverse side of the membrane. We consider the coupling of the cantilever to a two-level system composed of the  $^{87}\text{Rb}$  hyperfine sub-levels  $|F = 2, m_F = 2\rangle$  and  $|F = 2, m_F = 1\rangle$ . The Hamiltonian describing this coupled atom-cantilever system is [15]  $H = \hbar\omega_c(n + \frac{1}{2}) + \hbar\omega_L\hat{S}_y + H_{\text{int}}$ , where  $H_{\text{int}} = \mu_B g_F G_m z F_z \approx \hbar g_{\text{eff}}(S^+ a^- + S^- a^+)$ , and we have not explicitly included the potential associated with the optical confinement or motional degrees of freedom of the atoms. The effective single-atom single-phonon Rabi frequency  $g_{\text{eff}} \equiv g_F G_m z_{qm} \mu_B / \hbar$  satisfies the strong-coupling condition for the proposed experimental parameters (see Fig. 3).

The controlled-not (CNOT) gate using the coupled atom-cantilever system is analogous to that proposed and demonstrated for trapped ions [26, 27]. The qubits consist of the internal atomic spin states  $|\uparrow\rangle \equiv |F = 2, m_F = 1\rangle$  and  $|\downarrow\rangle \equiv |F = 1, m_F = -1\rangle$ , along with the cantilever vibrational states  $|0\rangle$  and  $|1\rangle$  corresponding to Fock states of the ground and first excited states, respectively. The atomic internal state  $|\text{aux}\rangle \equiv |F = 2, m_F = 2\rangle$  is used as an auxiliary state. By adjusting the background magnetic field, the transition frequency  $\omega_{2,1}$  between  $|\text{aux}\rangle$  and  $|\uparrow\rangle$  can be brought into, and out of, resonance with the fundamental mode of the cantilever.

The non-linear Zeeman shift in a background magnetic field of  $160 \mu\text{T}$  separates  $\omega_{2,1}$  from  $\omega_{1,0} \equiv |2, 1\rangle \rightarrow |2, 0\rangle$  by approximately 360 Hz.

For the gate sequence, first a  $\pi/2$  pulse is applied to the spin-only component of the wave function, using a semiclassical microwave or Raman transition with interaction Hamiltonian  $H_{\text{hf}} = \frac{\hbar\Omega}{2} [|\downarrow\rangle\langle\uparrow|e^{-i\phi} + |\uparrow\rangle\langle\downarrow|e^{i\phi}]$ , for a time  $\pi/(2\Omega)$  and laser phase  $\phi = \pi/2$ , resulting in the transformation  $|\uparrow\rangle \rightarrow \frac{1}{\sqrt{2}}(|\uparrow\rangle - |\downarrow\rangle)$ ,  $|\downarrow\rangle \rightarrow \frac{1}{\sqrt{2}}(|\uparrow\rangle + |\downarrow\rangle)$ . Then the magnetic field is ramped so that the cantilever resonance frequency matches  $\omega_{2,1}$ , and the two are allowed to interact for the duration of a  $2\pi$  pulse. For the atom in state  $|\uparrow\rangle$ , if the cantilever is in its ground state, no interaction occurs, while if the cantilever is in the excited state, after the  $2\pi$  pulse, the state will acquire a minus sign:  $|\uparrow\rangle|0\rangle \rightarrow |\uparrow\rangle|0\rangle$ ,  $|\uparrow\rangle|1\rangle \rightarrow -|\uparrow\rangle|1\rangle$ . Finally, a  $-\pi/2$  pulse is applied to the spin-only component of the wave function, completing the CNOT operation.

The atoms in the optical lattice can act as ‘slow flying qubits’, and allow selective long-range entanglement between cantilevers in a planar geometry. We assume an initial state  $|\text{aux}\rangle|0\rangle|0\rangle$ . The magnetic field in the trap is brought into resonance with a cantilever at frequency  $\omega_{c1}$ , and the interaction is allowed to occur for the duration of a  $\pi/2$  pulse. The resulting state is the superposition  $\frac{1}{\sqrt{2}}(|\text{aux}\rangle|0\rangle|0\rangle - |\uparrow\rangle|1\rangle|0\rangle)$ . At this point the optical lattice is translated so the atom under consideration is centered over a second cantilever with frequency  $\omega_{c2}$ . The magnetic background field is shifted to bring this cantilever into resonance with the Zeeman transition  $\omega_{2,1}$ , and they are allowed to interact for the duration of a  $\pi$  pulse. The final state becomes  $-\frac{i}{\sqrt{2}}|\uparrow\rangle[|0\rangle|1\rangle + |1\rangle|0\rangle]$ , so that the vibrational states of the cantilevers are in an entangled superposition, despite their differing resonant frequencies and relatively large spatial separation.

*Noise sources, Loss and Decoherence.* We assume a cantilever with  $Q = 3 \times 10^5$  at 1.1 MHz, which has a dissipation rate  $\kappa/(2\pi)$  of 1.8 Hz. Experimentally,  $Q$  factors as high as  $3.8 \times 10^5$  have recently been achieved at low temperature for cantilevers with resonance frequencies of order  $\sim 1$  MHz [28]. The cantilever decoherence time  $\tau_c$  considered alone limits the atom-cantilever CNOT gate fidelity to roughly  $\sim e^{-t_g/\tau_c} \approx 0.87$  for a gate operation time  $t_g = 80$  ms (for  $g_{\text{eff}}/2\pi = 12.7$  Hz), and is expected to be a dominant source of infidelity.

The atomic states involved with the controlled phase gate:  $|\uparrow\rangle$  and  $|\text{aux}\rangle$ , are susceptible to longitudinal magnetic de-phasing. If  $\delta\mu_{\parallel} \approx \mu_B/2$  is the residual magnetic moment difference between the states in the background magnetic field, the rate of de-phasing can be estimated as  $\tau_{\parallel} \sim \hbar/(\delta\mu_{\parallel}\Delta B_{\parallel})$  for a magnetic field fluctuation  $\Delta B_{\parallel}$  at frequencies comparable to or less than the inverse gate operation time [29]. For longitudinal magnetic background field fluctuations at the  $\sim 0.1$  nT level, the de-phasing rate  $\tau_{\parallel}^{-1}$  is approximately

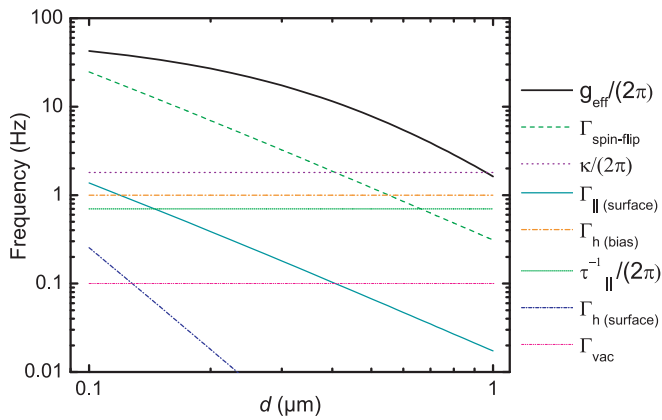


FIG. 3: (Color online) Rabi frequency  $g_{\text{eff}}/(2\pi)$  and decoherence or loss rates as described in the text versus atom-surface separation  $d$ . We include  $\Gamma_{\text{vac}}$  for the estimated atomic background loss. At  $d = 375$  nm the ratio of Rabi frequency to the discussed decoherence or loss mechanisms is close to maximal.

0.7 Hz. The longitudinal spectrum of thermal magnetic field noise at low frequency is estimated [30, 31] as  $S_{B\parallel}(\omega = 0) = \frac{\mu_0^2}{32\pi} \frac{k_B T \sigma h}{d(d+h)}$  for a metal of thickness  $h$  at distance  $d$  above the surface. This leads to a de-phasing rate  $\Gamma_{\parallel \text{surface}} \sim (\delta\mu_{\parallel})^2 S_{B\parallel} / 2\hbar^2$ , where  $S_{B\parallel}$  is the noise spectrum of longitudinal magnetic field noise [29, 30]. The de-phasing rate for 30 nm of Pt with conductivity  $\sigma^{-1} = 10.6 \times 10^{-8} \text{ ohm}^{-1}\text{m}^{-1}$  at  $T = 300$  K is shown in Fig. 3. Use of a metal with higher resistivity could be beneficial. Cooling the surface may be helpful provided the metal layer exhibits a sub-linear dependence of resistivity on temperature. Such properties may be attainable by using suitable metallic alloys.

Transverse magnetic field noise at or near the atomic Larmor frequency can result in Zeeman spin-flip transitions with a rate [32]  $\Gamma_{if}(d, \omega_L) = \Sigma_{\alpha} \frac{\mu_B^2 g_S^2 \langle i|\mu_{\alpha}|f\rangle^2}{\hbar^2} S_B^{\alpha\alpha}(d; \omega_L)$ . Here the initial and final states  $|i\rangle$  and  $|f\rangle$  are of the form  $|F, m\rangle$ ,  $|F, m \pm 1\rangle$ , and  $\vec{\mu} = \mu_B g_F \vec{F}$ . For the regime we consider, where the skin-depth at the Larmor frequency ( $\sim 100 \mu\text{m}$  at 1 MHz) is much larger than the metal thickness  $h$ , the spectral density of magnetic field noise can be expressed as [31]  $S_{B\perp}(d; \omega_L) = \frac{k_B T \sigma \mu_0^2}{16\pi} \left[ \frac{h}{d(d+h)} \right] = 2S_{B\parallel}$ . The estimated spin-flip rate  $\Gamma_{\text{spin-flip}}$  is shown in Fig. 3. The rates are somewhat slower than that ordinarily obtained for microchip traps below  $1 \mu\text{m}$  since the thickness of the metal layer is taken to be only 30 nm. This is permissible since the metal does not need to carry the relatively large electric currents needed for magnetic trapping on atom chips. This feature represents a main advantage of the proposed optical confinement scheme.

The heating rate from the trap ground state to its first excited vibrational state by near-field noise can be estimated for a thin metallic plane as  $\Gamma_{h(\text{surface})} \approx$

$\frac{\mu_{\parallel}^2}{\hbar^2} \frac{z_{qm}^2}{d^2} S_{B\parallel}(d; \omega_t) \approx \frac{\mu_{\parallel}^2}{\hbar^2} \frac{a_{qm}^2}{d^2} \frac{k_B T \sigma \mu_0^2}{16\pi} \left[ \frac{h}{d(d+h)} \right]$ , following Ref. [30]. Fluctuations in the bias fields can result in heating at a rate [30]  $\Gamma_{h(\text{bias})} = \frac{m_{\text{RB}} \omega^3}{2\hbar} S_h$ , where  $S_h$  is the spectrum of trap height fluctuations at the trap frequency. For a bias field fluctuation of 0.1 nT, the corresponding heating rate is  $\approx 1$  Hz.

We have identified a possible use for cantilevers in the context of quantum computation with neutral atoms in an optical lattice. Also we have described a scheme for the realization of a controlled-NOT gate in a hybrid atomic-mechanical system. A gate fidelity approaching 90 % may be possible with the given experimental parameters. Though significant experimental advances are required to realize the quantum gate or entanglement protocols discussed in this work, they may be possible within a few years. The system may provide a novel testing ground for coherence in macroscopic quantum systems. Higher gate fidelities could be achieved by employing higher  $Q$  resonators or by using tailored materials to improve the near-field magnetic noise environment. For example,  $Q$  factors in the  $10^7$  range have been observed [5] in different but similar micro-mechanical systems.

We acknowledge helpful discussions with E. Knill, D. Wineland, J. Home, and A. Ludlow. This work of NIST, an agency of the U.S. government, is not subject to copyright. AG acknowledges support from the NRC.

\* aageraci@boulder.nist.gov

- [1] A. Naik *et al.*, Nature **443** 193 (2006).
- [2] J. D. Teufel *et al.*, Phys. Rev. Lett. **101**, 197203 (2008).
- [3] O. Arcizet *et al.*, Nature **444** 71 (2006).
- [4] Claudiu Genes *et al.*, Phys. Rev. **A 77**, 033804 (2008).
- [5] J. D. Thompson *et al.*, Nature **452** 72 (2006).
- [6] D. Kleckner and D. Bouwmeester, Nature **444**, 75 (2006).
- [7] M. Poggio *et al.*, Phys. Rev. Lett. **99**, 017201 (2007).
- [8] A. Schliesser *et al.*, Nature Phys. **4** 415 (2008).
- [9] W. Marshall *et al.*, Phys. Rev. Lett. **91** 130401 (2003).
- [10] J. Eisert *et al.*, Phys. Rev. Lett. **93** 190402 (2004).
- [11] A.D. Armour, M.P. Blencowe, and K.C. Schwab, Phys. Rev. Lett. **88** 148301 (2002).
- [12] A.D. Armour and M.P. Blencowe, New J. Phys. **10**, 095004 (2008), A.D. Armour and M.P. Blencowe, New J. Phys. **10**, 095005 (2008).
- [13] P. Rabl *et al.*, arXiv:0806.3606
- [14] Y. Lin *et al.*, Phys. Rev. Lett. **92** 050404 (2004).
- [15] P. Treutlein *et al.*, Phys. Rev. Lett. **99**, 140403 (2007).
- [16] Y. Miroshnychenko *et al.* Nature **442** 151 (2006), K.D. Nelson *et al.*, Nature Phys. **3** 556 (2007), P. Lee *et al.* Phys. Rev. Lett. **99**, 020402 (2007).
- [17] Y.-J. Wang *et al.*, Phys. Rev. Lett. **97**, 227602 (2006).
- [18] D. Rugar *et al.*, Nature **430**, 329-332 (2004).
- [19] G. K. Brennen *et al.*, Phys. Rev. Lett. **82** 1060 (1999).
- [20] O. Mandel *et al.*, Nature **425**, 937 (2003), I. Bloch, Nature **453**, 1016 (2008).
- [21] P. Treutlein *et al.*, Fortschr. Phys. **54**, 702-718 (2006).
- [22] H.B.G. Casimir and P. Polder, Phys. Rev. **73**, 360 (1948).

- [23] P. Treutlein *et. al.*, Phys. Rev. **A** **74** 022312 (2006).
- [24] J. Beugnon *et. al.*, Nat. Phys. **3** 696 (2007).
- [25] M. Anderlini, *et. al.*, Nature **448** 452 (2007).
- [26] J.I.Cirac and P.Zoller, Phys. Rev. Lett. **74** 4091 (1995).
- [27] C. Monroe *et. al.*, Phys. Rev. Lett. **75** 4714 (1995).
- [28] C. Degen, private communication
- [29] A. Stern, Y. Aharonov, and Y. Imry, Phys. Rev. **A** **41** 3436 (1990).
- [30] C. Henkel *et. al.*, Appl. Phys. **B** (2002).
- [31] T. Varpula, and T. Poutanen, J. Appl. Phys. **55** 4015 (1984).
- [32] C. Henkel *et. al.*, Appl. Phys. B **69** 379 (1999).